The effect of normal and insulating layers on 0- transitions in Josephson junctions with a ferromagnetic barrier

2015 New J. Phys. 17 113022

(http://iopscience.iop.org/1367-2630/17/11/113022)

IOP Publishing New J. Phys. 17 (2015) 113022 doi:10.1088/1367-2630/17/11/113022

New Journal of Physics
The open access journal at the forefront of physics

Deutsche Physikalische Gesellschaft DPG
IOP Institute of Physics

Published in partnership with: Deutsche Physikalische Gesellschaft and the Institute of Physics

OPEN ACCESS

RECEIVED
7 July 2015

REVISED
6 September 2015

ACCEPTED FOR PUBLICATION
8 September 2015

PUBLISHED
5 November 2015

PAPER

The effect of normal and insulating layers on 0-π transitions in Josephson junctions with a ferromagnetic barrier

D M Heim[1], N G Pugach[2,3], M Yu Kupriyanov[2,4], E Goldobin[5], D Koelle[5], R Kleiner[5], N Ruppelt[6], M Weides[7] and H Kohlstedt[6]

[1] Institut für Quantenphysik and Center for Integrated Quantum Science and Technology (IQST), Universität Ulm, D-89069 Ulm, Germany
[2] Skobeltsyn Institute of Nuclear Physics, Lomonosov Moscow State University, 119991 Leninskie Gory, Moscow, Russia
[3] Royal Holloway University of London, Egham, Surrey, TW20 0EX, UK
[4] Moscow Institute of Physics and Technology, Dolgoprudny, Moscow Region, Russia
[5] Physikalisches Institut and Center for Quantum Science (CQ) in LISA^{+}, Universität Tübingen, D-72076 Tübingen, Germany
[6] Nanoelektronik, Technische Fakultät, Christian-Albrechts-Universität zu Kiel, D-24143 Kiel, Germany
[7] Physikalisches Institut, Karlsruhe Institute of Technology, D-76131 Karlsruhe, Germany

E-mail: dennis.heim@uni-ulm.de **and** koelle@uni-tuebingen.de

Keywords: superconductivity, Josephson effects, tunneling phenomena, multilayers, heterostructures, proximity effects

Abstract

Using the Usadel approach, we provide a formalism that allows us to calculate the critical current density of 21 different types of Josephson junctions (JJs) with a ferromagnetic (F) barrier and additional insulating (I) or/and normal (N) layers inserted between the F layer and superconducting (S) electrodes. In particular, we obtain that in SFS JJs, even a thin additional N layer between the S layer and F layer may noticeably change the thickness d_F of the F layer at which the 0-π transitions occur. For certain values of d_F, a 0-π transition can even be achieved by changing only the N layer thickness. We use our model to fit experimental data of SIFS and SINFS tunnel junctions.

1. Introduction

Superconducting spintronics is an intensively developing field [1]. It is based on the effects resulting from the competition and coexistence of magnetic and superconducting ordering. The mixing of spin and charge degrees of freedom with superconducting correlations in hybrid nanostructures leads to a rich spectrum of unusual physical phenomena [2–4]. Moreover, a new generation of supercomputers has been developed based on superconducting spintronics [5, 6]. One of the main goals of the recent superconducting spintronics development is the creation of rapid single flux quantum logic (RSFQ) elements, such as Josephson phase batteries [7–12] and magnetic memory [13–23]. Both, Josephson phase batteries and magnetic memory are based on ferromagnetic Josephson junctions (FJJs).

We consider an FJJ consisting of two thick superconducting (S) electrodes with a ferromagnetic (F) film between them; see figure 1(a). This canonical arrangement was considered in many theoretical works [2, 3]. The key property of this structure is the possibility of having negative critical current density J_c in some ranges of F layer thickness d_F. The transition from positive to negative J_c corresponds to the transition from the 0 to the π ground state of the JJ. For applications, one tries to choose such a thickness d_F, for which the (absolute) value of J_c in the π domain is as high as possible. This is usually the case inside the first π domain along the F axis. For the simple SFS structure, shown in figure 1(a), the boundaries of π domains and the whole $J_c(d_F)$ dependence is known [24].

However, experimental π JJs often include extra insulating (I) layers [25, 26] and/or normal (N) layers [26, 27] between SF or FS layers. The purpose of the additional I layer(s) is to enlarge the characteristic voltage, especially in the π state. It was shown [28, 29] that the presence of extra insulating layers shifts the first 0-π transition to smaller values of d_F. There are also several reasons to consider N layer(s), as follows.

First, a so-called 'dead' layer exists in many sputtered ferromagnetic films. The dead layer is a surface layer of the ferromagnet, which behaves as a non-magnetic metal. It usually appears due to the surface roughness or the

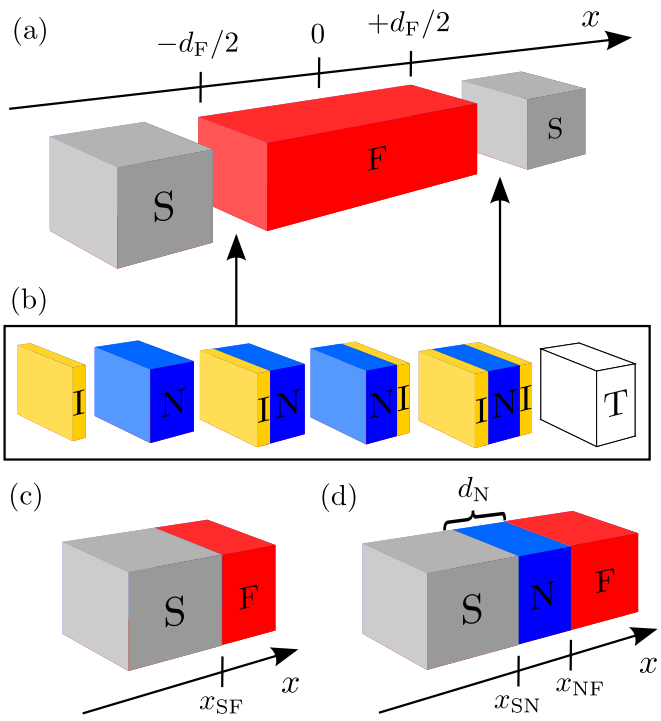

Figure 1. The Josephson junction configurations we consider. In (a) we show the basic geometry consisting of two thick superconducting (S) electrodes separated by a ferromagnetic (F) weak link of thickness d_F. Our formalism covers all 21 Josephson junctions resulting from the insertion of one of the layers shown in (b) at the SF interfaces in (a). These layers are composed of insulating (I) or normal metal (N) films. The case of no additional layer is denoted by T (transparent interface). In (c) and (d) we define parameters for the derivation of our formalism.

mutual dissolution of atoms at the interface between N and F layers. Such a dead layer is inherent, for example in NF interfaces involving Cu and its alloys with 3*d* metals, which are very popular as spacers. Usually it is naively assumed that the dead layer makes the effective F layer thinner and adds an extra N layer (non-magnetic F). Many experimental data match the theory only if one assumes such a dead layer of finite thickness [24, 26, 30–34]. However, sometimes such a naive fit gives questionable results because it does not take into account the correct boundary conditions at all interfaces.

Second, an N layer between F and S is often technologically necessary to produce high-quality JJs [24, 26, 27, 30–33, 35–38], for example by preventing diffusion between F and S films [39]. The presence of an N layer in FJJs was not taken into account in any theoretical work [44, 40–43, 45] (see also [2, 3] for review) in spite of numerous experiments. We show that this is reasonable only if the F and N metals behave fully identically, except for their magnetic properties. Otherwise, the presence of the thin N layer changes the boundary conditions, which affects the dependence of the Josephson current J_c on d_F. Recent experiments [46], which use a new continuous *in situ* technology allowing the deletion of this layer, actually exhibit a change of the 0-π transition points in the $J_c(d_F)$ dependence.

The overall effect of these extra I and N layers is not studied in detail. Therefore, we present a formalism in the following, which allows us to calculate the critical current density of FJJs with additional I and/or N layers inserted between SF and/or FS layers. The heterostructures under question can be constructed by selecting one of the items of figure 1(b) and inserting it by following one of the arrows into figure 1(a). At the other arrow position we insert either the same or another item from figure 1(b). In this way we obtain 21 possible configurations of layers in FJJs.

The article is organized as follows. In section 2 we describe our model based on the Usadel equations supplemented with Kupriyanov–Lukichev boundary conditions. Different types of interlayer boundaries are analysed. Section 3 presents the obtained dependencies of the critical current density on the F layer thickness as well as the analysis of the 0-π transitions in the framework of a linear approximation. We use our formalism in section 4 to fit experimental data of SINFS and SIFS junctions. Section 5 concludes this work. Details of the calculation can be found in the appendix.

2. Model

2.1. The boundary value problem

The basic Josephson junction configuration we consider is sketched in figure 1(a). It consists of two thick S electrodes enclosing an F layer of the thickness d_F along the x axis. Our model allows to consider an additional I or N layer at the SF interfaces as well as I layers at the SN or NF interfaces, as illustrated by figure 1(b).

We calculate the critical current density J_c of these configurations by determining their Green's functions in the 'dirty' limit. In this limit, the elastic electron scattering length is much smaller than the characteristic decay length of the superconducting wave function. We determine the Green's functions with the help of the Usadel equations [47], which we use similar to [3] in the form

$$\xi_j^2\left(G_j\frac{\partial^2}{\partial x^2}F_j - F_j\frac{\partial^2}{\partial x^2}G_j\right) - \left(\widetilde{\Omega} + \eta\, G_j\right)F_j = 0,$$
$$G_j^2 + F_j\widetilde{F}_j = 1, \quad j \in \{\mathrm{N}, \mathrm{F}\}, \tag{1}$$

in the N and F layer, where F_j and G_j are the Usadel Green's functions, while $\widetilde{F}_j(\omega) \equiv F_j^*(-\omega)$. The frequencies $\widetilde{\Omega} \equiv \Omega + ih$ contain the scaled Matsubara frequencies $\Omega \equiv \omega/(\pi T_c)$, where $\omega \equiv \pi T(2n+1)$ at the temperature T, and T_c is the critical temperature of the superconductor. By using the definition $\eta \equiv 1/(\tau_m \pi T_c)$ we take, similar to [28], the spin-flip scattering time τ_m into account. This approach requires a ferromagnet with strong uniaxial anisotropy, for example, Cu alloys with transition metals, which are used in many experiments. Equation (1) should be satisfied for any integer number n. The scaled exchange energy $h \equiv H/(\pi T_c)$ of the ferromagnetic material, where the energy H describes the exchange integral of the conducting electrons, is assumed to be zero in the N layer.

In our model we use the coherence lengths

$$\xi_N \equiv \sqrt{\frac{D_N}{2\pi T_c}}, \quad \xi_F \equiv \sqrt{\frac{D_F}{2\pi T_c}}, \quad \xi_H \equiv \sqrt{\frac{D_F}{H}} \tag{2}$$

of the superconducting correlations, which are defined with the help of the diffusion coefficients D_N and D_F in the normal and ferromagnetic metal, respectively. We use the scaling defined by $\hbar \equiv k_B \equiv 1$.

The decay length ξ_H of superconducting correlations in the ferromagnet is usually in the order of nm. This is sufficiently small ($\xi_H \lesssim d_F$) to consider the supercurrent as a result of interference of anomalous Green's functions induced from the superconducting banks. It was shown [28] that this ansatz is valid even for small distances $d_F \sim \xi_H$, that is, in the region of the first 0-π transition.

It is convenient to consider this problem in theta parametrization [48]

$$F_j = e^{i\varphi_j}\sin\theta_j, \quad G_j = \cos\theta_j, \tag{3}$$

where φ_j is independent of the coordinate x. It corresponds to the phase $\varphi_j \equiv \pm\phi/2$ of the order parameter of the S banks for the right and left superconducting electrode, respectively, while θ_j satisfies the sine-Gordon–type differential equation

$$\xi_j^2\frac{\partial^2}{\partial x^2}\theta_j - \left(\widetilde{\Omega} + \eta\cos\theta_j\right)\sin\theta_j = 0. \tag{4}$$

Since we assume that the superconductivity in the S electrodes is not suppressed by the neighbouring N and F layers, we obtain

$$\theta_S = \arctan\frac{\Delta}{\omega} \tag{5}$$

analogous to Vasenko *et al* [28] at the interfaces of the superconductor, where Δ is the absolute value of the order parameter in the superconductor. The validity of this assumption depends on the values of the suppression parameters

$$\gamma_{BSF} \equiv \frac{R_{BSF}A_{BSF}}{\rho_F\xi_F}, \quad \gamma_{SF} \equiv \frac{\rho_S\xi_S}{\rho_F\xi_F},$$
$$\gamma_{BSN} \equiv \frac{R_{BSN}A_{BSN}}{\rho_N\xi_N}, \quad \gamma_{SN} \equiv \frac{\rho_S\xi_S}{\rho_N\xi_N} \tag{6}$$

at the S boundaries, which we discuss in more detail in subsection 2.3. We use the resistances R_{BSF}, R_{BSN} and the areas A_{BSF}, A_{BSN} of the SF and SN interfaces. The values ρ_N, ρ_F and ρ_S describe the resistivity of the N, F and S metals, respectively.

The Kupriyanov–Lukichev boundary condition [49, 50] at the superconducting interface, shown in figure 1(c), is

$$\sin\left(\theta_{\mathrm{F,S}} - \theta_{\mathrm{S}}\right) = \gamma_{\mathrm{BSF}}\xi_{\mathrm{F}}\left[\frac{\partial}{\partial x}\theta_{\mathrm{F}}\right]_{x_{\mathrm{SF}}}, \tag{7}$$

where $\theta_{\mathrm{F,S}} \equiv \theta_{\mathrm{F}}(x_{\mathrm{SF}})$, while in figure 1(d) it is

$$\sin\left(\theta_{\mathrm{N,S}} - \theta_{\mathrm{S}}\right) = \gamma_{\mathrm{BSN}}\xi_{\mathrm{N}}\left[\frac{\partial}{\partial x}\theta_{\mathrm{N}}\right]_{x_{\mathrm{SN}}}, \tag{8}$$

where $\theta_{\mathrm{N,S}} \equiv \theta_{\mathrm{N}}(x_{\mathrm{SN}})$, at the SN boundary and

$$\sin\left(\theta_{\mathrm{F,N}} - \theta_{\mathrm{N,F}}\right) = \gamma_{\mathrm{BNF}}\xi_{\mathrm{F}}\left[\frac{\partial}{\partial x}\theta_{\mathrm{F}}\right]_{x_{\mathrm{NF}}} \tag{9}$$

at the NF boundary. Here we defined $\theta_{\mathrm{F,N}} \equiv \theta_{\mathrm{F}}(x_{\mathrm{NF}})$ and $\theta_{\mathrm{N,F}} \equiv \theta_{\mathrm{N}}(x_{\mathrm{NF}})$. Additionally, we use the differentiability condition

$$\gamma_{\mathrm{NF}}\xi_{\mathrm{F}}\left[\frac{\partial}{\partial x}\theta_{\mathrm{F}}\right]_{x_{\mathrm{NF}}} = \xi_{\mathrm{N}}\left[\frac{\partial}{\partial x}\theta_{\mathrm{N}}\right]_{x_{\mathrm{NF}}}. \tag{10}$$

The suppression parameters

$$\gamma_{\mathrm{BNF}} \equiv \frac{R_{\mathrm{BNF}}A_{\mathrm{BNF}}}{\rho_{\mathrm{F}}\xi_{\mathrm{F}}}, \quad \gamma_{\mathrm{NF}} \equiv \frac{\rho_{\mathrm{N}}\xi_{\mathrm{N}}}{\rho_{\mathrm{F}}\xi_{\mathrm{F}}} \tag{11}$$

are defined analogous to (6), but not restricted to only small or large values.

In order to finally extract the critical current density J_{c} from the current phase relation $J(\phi) = J_{\mathrm{c}}\sin\phi$ we will calculate the total current density [2]

$$J(\phi) = \mathrm{i}\frac{\pi T}{2e\rho_{\mathrm{F}}}\sum_{\omega=-\infty}^{\infty}\left[F_{\mathrm{F}}(\omega)\,\frac{\partial}{\partial x}F_{\mathrm{F}}^{*}(-\omega) - F_{\mathrm{F}}^{*}(-\omega)\,\frac{\partial}{\partial x}F_{\mathrm{F}}(\omega)\right]_{x=0} \tag{12}$$

flowing through our device, with the help of the Green's function F_{F} in the F layer. Here we chose the position $x = 0$; see figure 1(a), in order to simplify the calculation.

2.2. Critical current density

In this section we rewrite expression (12) to be able to directly calculate the critical current densities of all SFS Josephson junctions of the type sketched in figure 1(a), which may include each of the layers, shown in figure 1(b) at the SF interfaces.

In order to solve the Usadel equations (1) in the F layer we use the ansatz [28, 51]

$$F_{\mathrm{F}}(x) = \mathrm{e}^{-\mathrm{i}\phi/2}\sin\left[\theta_{\mathrm{F}}^{-}(x)\right] + \mathrm{e}^{+\mathrm{i}\phi/2}\sin\left[\theta_{\mathrm{F}}^{+}(x)\right], \tag{13}$$

where each function $\theta_{\mathrm{F}}^{-}(x)$ and $\theta_{\mathrm{F}}^{+}(x)$ solves the non-linear differential equation (4) for $j = F$. Additionally we use the conditions $\theta_{\mathrm{F}}^{\pm} = 0$ and $\partial\theta_{\mathrm{F}}^{\pm}/\partial x = 0$ at $x = \mp\infty$. Then the solution $\theta_{\mathrm{F}}^{-}(x)$ will turn out to be most dominant in the left side of the F part and to decay exponentially in the right side of the junction. Therefore, it has practically no overlap with the solution $\theta_{\mathrm{F}}^{+}(x)$ which is dominant in the right side of the F layer.

We obtain both solutions $\theta_{\mathrm{F}}^{-}(x)$ and $\theta_{\mathrm{F}}^{+}(x)$ by integrating the differential equation (4) for $j = F$ twice. The first integration results in

$$\frac{\partial}{\partial x}\theta_{\mathrm{F}}^{\pm} = \pm\frac{2}{\xi_{\mathrm{F}}}\sqrt{\widetilde{\Omega} + \eta\cos^{2}\frac{\theta_{\mathrm{F}}^{\pm}}{2}}\,\sin\frac{\theta_{\mathrm{F}}^{\pm}}{2}, \tag{14}$$

where $\theta_{\mathrm{F}}^{\pm} \equiv \theta_{\mathrm{F}}^{\pm}(x)$. A second integration leads us, by using the definition $q \equiv \sqrt{\widetilde{\Omega} + \eta}$, to the equation [28, 52]

$$\frac{\sqrt{\widetilde{\Omega} + \eta\cos^{2}\frac{\theta_{\mathrm{F}}^{\pm}}{2}} - q\cos\frac{\theta_{\mathrm{F}}^{\pm}}{2}}{\sqrt{\widetilde{\Omega} + \eta\cos^{2}\frac{\theta_{\mathrm{F}}^{\pm}}{2}} + q\cos\frac{\theta_{\mathrm{F}}^{\pm}}{2}} = g^{\pm}\exp\left[\pm\frac{2q}{\xi_{\mathrm{F}}}\left(x \mp \frac{d_{\mathrm{F}}}{2}\right)\right]. \tag{15}$$

Here $g^{\pm}$ are the integration constants. In the F layer we can assume small superconducting correlations $\theta_{\mathrm{F}} \ll 1$ to linearise the denominator of the left-hand side of (15), which leads us to the equation

$$\sin\frac{\theta_{\mathrm{F}}^{\pm}(x)}{2} = \chi^{\pm}\exp\left[\pm\frac{q}{\xi_{\mathrm{F}}}\left(x \mp \frac{d_{\mathrm{F}}}{2}\right)\right]. \tag{16}$$

The rewritten integration constants $\chi^{\pm}$ are given by the boundary conditions at the right and left ferromagnetic interfaces as

$$\chi^{+} \equiv \sin\frac{\theta_{\mathrm{F}}\left(+d_{\mathrm{F}}/2\right)}{2}, \quad \chi^{-} \equiv \sin\frac{\theta_{\mathrm{F}}\left(-d_{\mathrm{F}}/2\right)}{2}. \tag{17}$$

By inserting the ansatz (13) with the solutions (16) into the current density (12), and by using the approximation $\widetilde{\Omega} \approx ih$, which holds for the condition $\pi T_{\mathrm{c}} \ll H$ and the assumption $\xi_{\mathrm{H}} \lesssim d_{\mathrm{F}}$, we obtain the critical current density

$$J_{\mathrm{c}} = 16\frac{\pi T}{e\rho_{\mathrm{F}}}\sum_{\omega>0}\mathrm{Re}\left(\gamma\ \mathrm{e}^{-\gamma d_{\mathrm{F}}}\chi^{+}\ \chi^{-}\right), \quad \gamma = \frac{q}{\xi_{\mathrm{F}}}. \tag{18}$$

The constants $\chi^{\pm}$ will be determined in the next section.

2.3. SF interface without or including an N layer

In the following we determine a constant χ_{TI} to replace χ^{+} or χ^{-} in (18) in the case of no N layer at an SF interface, as shown for example in figure 1(c). The index TI stands for transparent or insulating.

We insert the integrated sine-Gordon equation (14) at the position x_{SF} into the boundary condition (7) and obtain the relation

$$2\gamma_{\mathrm{BSF}}\sqrt{\widetilde{\Omega} + \eta\cos^{2}\frac{\theta_{\mathrm{F,S}}}{2}}\ \sin\frac{\theta_{\mathrm{F,S}}}{2} = \sin\left(\theta_{\mathrm{S}} - \theta_{\mathrm{F,S}}\right). \tag{19}$$

By defining $\chi_{\mathrm{TI}} \equiv \sin(\theta_{\mathrm{F,S}}/2)$ analogous to (17), we rewrite (19) in the form

$$\begin{aligned}
&\chi_{\mathrm{TI}}^{4} + 2\gamma_{\mathrm{BSF}}\sqrt{\widetilde{\Omega} + \eta\left(1-\chi_{\mathrm{TI}}^{2}\right)}\sin\theta_{\mathrm{S}}\,\chi_{\mathrm{TI}}^{3} \\
&+ \left\{\gamma_{\mathrm{BSF}}^{2}\left[\widetilde{\Omega} + \eta\left(1-\chi_{\mathrm{TI}}^{2}\right)\right] - 1\right\}\chi_{\mathrm{TI}}^{2} \\
&- \gamma_{\mathrm{BSF}}\sqrt{\widetilde{\Omega} + \eta\left(1-\chi_{\mathrm{TI}}^{2}\right)}\sin\theta_{\mathrm{S}}\,\chi_{\mathrm{TI}} \\
&+ \frac{1}{4}\sin^{2}\theta_{\mathrm{S}} = 0.
\end{aligned} \tag{20}$$

In the case $\eta \to 0$, which means neglecting the effect of spin-flip scattering, this equation is a quartic equation in χ_{TI} and therefore exactly solvable. To find the solutions in this case we use the function *solve* of the MATLAB software. Afterwards we make use of (19) to select one of the four solutions. In the case $\eta \neq 0$ we solve (20) numerically by using the function *fsolve* of the MATLAB software together with the solution of the limit $\eta \to 0$ as the starting value.

In this way we find χ_{TI} for the determination of the critical current density (18) in the case of no N layer at the SF boundary. The case of a small parameter γ_{BSF} corresponds to a transparent SF interface, while a large one corresponds to an insulating interface [28, 52].

Next, we determine a constant χ_{N} for the case of a thin N layer $d_{\mathrm{N}} \ll \xi_{\mathrm{N}}$ between the superconductor and ferromagnet, as shown in figure 1(d).

By inserting the integrated sine-Gordon equation (14) for $x = x_{\mathrm{NF}}$ into the boundary condition (9), we obtain the equation

$$2\gamma_{\mathrm{BNF}}\sqrt{\widetilde{\Omega} + \eta\cos^{2}\frac{\theta_{\mathrm{F,N}}}{2}}\ \sin\frac{\theta_{\mathrm{F,N}}}{2} = \sin\left(\theta_{\mathrm{N,F}} - \theta_{\mathrm{F,N}}\right). \tag{21}$$

When we rewrite this equation using the definition $\chi_{\mathrm{N}} \equiv \sin(\theta_{\mathrm{F,N}}/2)$, the result

$$\begin{aligned}
&\chi_{\mathrm{N}}^{4} + 2\gamma_{\mathrm{BNF}}\sqrt{\widetilde{\Omega} + \eta\left(1-\chi_{\mathrm{N}}^{2}\right)}\sin\theta_{\mathrm{N,F}}\,\chi_{\mathrm{N}}^{3} \\
&+ \left\{\gamma_{\mathrm{BNF}}^{2}\left[\widetilde{\Omega} + \eta\left(1-\chi_{\mathrm{N}}^{2}\right)\right] - 1\right\}\chi_{\mathrm{N}}^{2} \\
&- \gamma_{\mathrm{BNF}}\sqrt{\widetilde{\Omega} + \eta\left(1-\chi_{\mathrm{N}}^{2}\right)}\sin\theta_{\mathrm{N,F}}\,\chi_{\mathrm{N}} \\
&+ \frac{1}{4}\sin^{2}\theta_{\mathrm{N,F}} = 0
\end{aligned} \tag{22}$$

looks similar to (20). The main difference is that it reduces in the case $\eta \to 0$ not to an equation of fourth order in χ_{N}. This is because we take an effect similar to the inverse proximity effect at the NF boundary into account; that is, the reduction of the superconducting correlations in the N layer due to the proximity of the F layer. Therefore, the value $\theta_{\mathrm{N,F}} \equiv \theta_{\mathrm{N}}(x_{\mathrm{NF}})$ also depends on χ_{N}, which itself is related to $\theta_{\mathrm{F,N}} \equiv \theta_{\mathrm{F}}(x_{\mathrm{NF}})$, even in the case $d_{\mathrm{N}} \ll \xi_{\mathrm{N}}$, as we show in the appendix.

However, we also show in the appendix that (22) reduces in the limit $\eta \to 0$ together with $\gamma_{\mathrm{NF}} \to 0$, which means assuming the conductivity of the N layer to be much larger than that of the ferromagnet, to an equation of

fourth order in χ_N. Therefore, we make three steps in order to solve (22). First we determine its solution in the case $\eta,\ \gamma_{NF} \to 0$ similar to the fourth-order case of (20). We then use this result as a starting value to solve (22) for only the limit $\eta \to 0$ with the help of the function *fsolve* of the MATLAB software. This in turn leads to another starting value which we use to solve (22) with *fsolve*, but without any limiting case.

The solution χ_N of (22) can finally be used as χ^+ or χ^- for the determination of the critical current density (18) in the case of an N layer at the SF interfaces. Small parameters γ_{BSN} and γ_{BNF} correspond to transparent SN and NF interfaces, while large ones correspond to insulating interfaces [28, 52].

3. Discussion

In this section we first select FJJ configurations, where the N layer has the largest influence. We then analyse their critical current densities with the help of the formalism we derived in the previous section. Finally, we discuss the results with the help of solutions of the linearised differential equation.

We do not analyse configurations where a thin N layer ($d_N \ll \xi_N$) is located between S and I layers, which gives only a negligible reduction of J_c compared to the case without an N layer. This is because the superconducting condensate simply penetrates into the whole N layer. The same effect occurs when the thin N spacer separates the S and F layers and both (SN and NF) interfaces are transparent.

However, when the SN boundary has a very weak transparency or gets even insulating, that is, when the N layer is located between an I and an F layer, then the N layer(s) play(s) a more notable role depending on the relation of resistances γ_{NF} (11), as we will see in the following.

Examples for the critical current density $J_c(d_F)$ in these situations are presented in figure 2 with different numbers of insulating barriers. To in- and exclude these barriers we use the boundary parameters shown in table 1. Since we only want to change N-layer properties, like $d_N,\ \rho_N$ or ξ_N of the same junction, we keep the product

$$\gamma_{BSN}\gamma_{NF} = \frac{R_{BSN}A_{BSN}}{\rho_F\xi_F} \tag{23}$$

constant.

Each section of figures 2(a)–(d) shows several dependences $J_c(d_F)$ for FJJs containing N layers of different thicknesses and the corresponding reference FJJ without any N layer (solid black lines [28, 53]). The I layers in all panels of figures 2(b)–(d), (f)–(h) are chosen to be exactly identical. Here we observe that the additional N layer at the IF boundary decreases the amplitude of J_c by 1–2 orders of magnitude and, while the insulating barrier at the SF boundary shifts the 0-π transitions towards smaller values of d_F (solid black lines), the additional N layer in the SINF part shifts it back to larger d_F.

This effect depends strongly on the value γ_{NF}, as can be seen from figures 2(f)–(h), where we show critical current densities $J_c(d_F)$ in the same FJJ configurations as in figures 2(b)–(d), but with fixed $d_N = 0.4\xi_N$ and variable $\gamma_{NF} = 1,\ 0.1,\ 0.01$. With decreasing γ_{NF}, the 0-π transitions are shifted back to their positions without an I layer. One may conclude that the thin N layer with small resistance ($\rho_N < \rho_F$) effectively 'smooths' the order parameter in the SIF region.

For a physical explanation of this behaviour, one can imagine that a decrease of the amplitude of the superconducting pair wave-function in the F layer is connected to a decrease of the function θ_F. In particular, the positions along the F layer where θ_F becomes zero correspond to sign reversals of the critical current density and are therefore directly linked to the thicknesses d_F where a 0-π transition occurs.

This picture already helps us to understand why an insulating layer at the SF interface shifts the 0-π transitions towards smaller values of d_F [28, 29]. This is because the I layer induces a decreasing shift to θ_F at the SF interface, as can be seen from (7) for $\gamma_{BSF} \gg 1$. Since θ_F decreases monotonically from the interfaces into the F layer, this shift results in a shift of its zeros towards the interface. This in turn leads to a shift of the 0-π transitions to smaller d_F, as can be seen by comparing, for example, the black lines in figures 2(a) and (b).

By inserting an N layer at the IF interface, we can mitigate this effect. In fact, the function θ is still decreased by the I layer, but the decrease of its derivative θ' may be smaller than in the case of a superconducting pair wave-function that directly penetrates the F layer. This in turn leads to a shift of the 0-π transition back to larger d_F.

To explain this effect, we replace the derivative θ'_N in (A.7) with the help of (10), which leads us to the derivative

$$\left[\frac{\partial\theta_F}{\partial x}\right]_{x_{NF}} = \frac{\Omega d_N}{\xi_N\xi_F\gamma_{NF}}\sin\theta_{N,S} - \frac{\sin\left(\theta_S - \theta_{N,S}\right)}{\gamma_{BSN}\gamma_{NF}\xi_F} \tag{24}$$

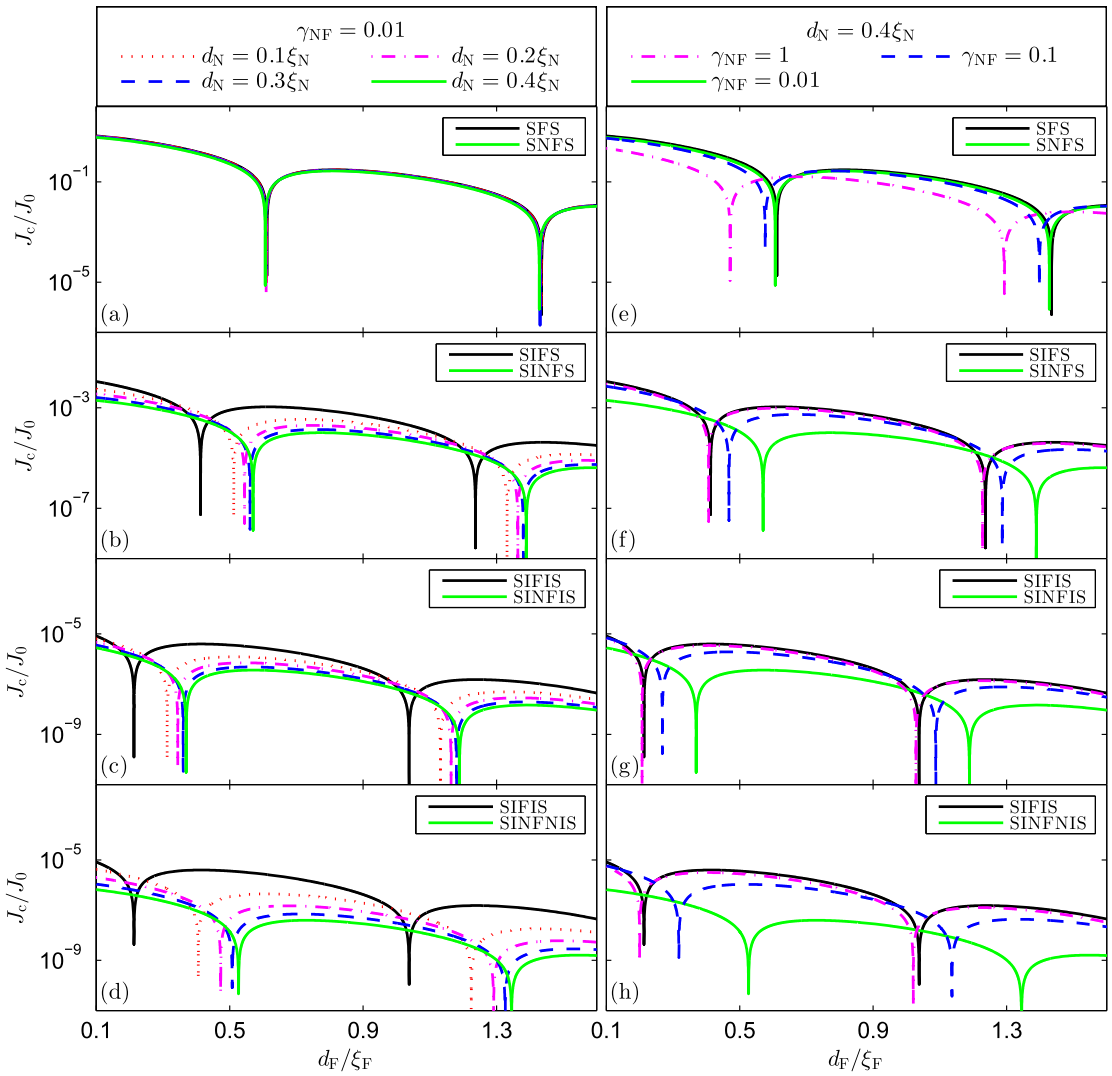

Figure 2. The critical current density $J_c(d_F)$ calculated using (18) for different FJJs in units of $J_0 = \pi T_c/(\rho_F \xi_F e)$. Coloured lines correspond to SFS junctions including N layers. The solid black lines are solutions without N layers and in agreement with [28, 51]. The coloured lines in figures (a)–(d) are dotted for $d_N = 0.1\xi_N$, dashed-dotted for $d_N = 0.2\xi_N$, dashed for $d_N = 0.3\xi_N$ and solid for $d_N = 0.4\xi_N$. Here we used the suppression parameter $\gamma_{NF} = 0.01$. In figures (e)–(h) the dashed-dotted lines correspond to $\gamma_{NF} = 1$, the solid lines to $\gamma_{NF} = 0.1$ and the dashed lines to $\gamma_{NF} = 0.01$ at the fixed thickness $d_N = 0.4\xi_N$. We used the suppression parameters given by table 1. Additionally we chose $h = 30$, $T_c = 9.2$ K, $T = 0.5T_c$ and $\eta = 0$. From figures (b)–(d) we conclude that inserting an N layer can mitigate the effect of the insertion of an I layer, and figures (f)–(h) show that this behaviour depends strongly on γ_{NF}.

Table 1. Parameters for the calculation of the critical current densities (18) shown in figure 2. The parameters γ_B are responsible for the presence of an I layer, while the equation for the calculation of $\chi^{\pm}$ determines whether we consider an N layer or not. We keep the product $\gamma_{BSN}\gamma_{NF}$ constant because its outcome (23) does not change during our analysis.

Interface	γ_{BSF}	γ_{BNF}	$\gamma_{BSN}\gamma_{NF}$	for $\chi^{\pm}$
SF	0.001	—	—	(20)
SIF	100	—	—	(20)
SNF	—	0.001	0.001	(22)
SINF	—	0.001	100	(22)

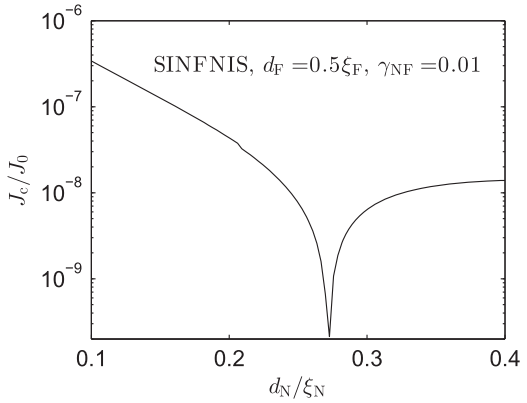

Figure 3. The critical current density $J_c(d_N)$ (18) in units of $J_0 = \pi T_c/(\rho_F \xi_F e)$ for FJJs in SINFNIS configuration. The F layer thickness $d_F = 0.5\xi_F$ is constant, while the thickness d_N of both N layers changes. In this way, we control the 0-π transition only by adjusting d_N. Analogous to figure 2(d), where the same FJJ configuration is analysed for varying d_F, we use the suppression parameters of table 1 and the parameters $h = 30$, $T_c = 9.2$ K, $T = 0.5T_c$, $\eta = 0$.

at the F interface. For $d_N = 0$, (24) resembles (7). Therefore, we obtain, by using the values defined in table 1, the correct limiting results. Note that θ'_F is negative in this case because the amplitude of the superconducting pair wave-function decreases when entering the F layer.

An increase of d_N increases θ'_F and therefore shifts the 0-π transitions towards larger d_F, as shown by figures 2(b)–(d). Furthermore, from (24) it can be understood why a smaller value of γ_{NF} induces a larger increase of θ'_F. This again shifts the 0-π transitions towards larger d_F, as shown by figures 2(f)–(h).

The same effect occurs in figure 2(e), but it has a different interpretation because the 0-π transitions are already shifted to large d_F without an N layer, due to the absence of the I layer (black line). A small value of γ_{NF} does not change this situation significantly. However, if γ_{NF} increases and therefore θ'_F decreases, the 0-π transitions get shifted to smaller d_F.

These effects are related partially to d_N that may be small ($d_N \ll \xi_N$) but mainly to the conducting properties of the N layer represented by γ_{NF} (11).

Note that we neglected the effect of spin-flip scattering in figure 2; that is, we chose $\eta = 0$. An increase of η shifts all shown 0-π transitions towards larger d_F, including the ones of junctions without an N layer [28, 52]. It is not necessary to consider this effect in order to understand the role of N layers in FJJs. However, the described effect is important for the fitting of experimental results in section 4.

The influence of N layers on FJJs can be seen most clearly when they are inserted at IF interfaces and d_F is kept constant, not far from a 0-π transition, while d_N changes. In this way, *the 0-π transition can be controlled by* d_N, as shown in figure 3. Here we consider an SIFIS junction which is in the 0 state for $d_F = 0.5\xi_F$. By adding N layers at the IF interfaces and increasing their thicknesses simultaneously, we tune the FJJ into the π regime. Figure 3 considers the same FJJ configuration as figure 2(d), where d_N is fixed and d_F changes.

To understand the role of the boundary parameters in the 0-π transition patterns in more detail, it is useful to analyse it in a simple linear approximation. This approximation can be used if both S electrodes have non-transparent interfaces, or if $T \to T_c$. Then we may assume that $\theta \ll 1$, $G = \cos\theta \approx 1$ and $F \sim \sin\theta \approx \theta$. The general solution of the Usadel equations (1) in the non-superconducting layers has the form $\exp(pmk_{N,F}x)$, where $k_N \equiv \sqrt{2\omega/D_N}$, $k_F \equiv \sqrt{2\tilde{\omega}/D_F} \equiv p + iq$, where p and q are real. The critical current density is given by the expression (12). For FJJs without an N layer, the critical current density has already been calculated in [28, 45, 52, 53].

3.1. Transparent-interface structures: SFS, SNFS, SNFNS

We start with the analysis of figures 2(a) and (e). For this purpose we assume that all interfaces are transparent, that is γ_{BSF}, γ_{BSN}, $\gamma_{BNF} \ll 1$, and $T \to T_c$. If $\gamma_{SF} \ll 1$, the critical current density of the SFS junction (cf solid black lines) reads [3]

$$J_c \sim \sum_{\omega} \left[\frac{\Delta^2}{\omega^2} \operatorname{Re} \frac{k_F}{\sinh\left(k_F d_F\right)} \right] \tag{25}$$

and the positions of the 0-π transitions are defined by the solutions of the equation

$$\tan\left(qd_{\mathrm{F}}\right) = -\frac{p}{q}\tanh\left(pd_{\mathrm{F}}\right). \tag{26}$$

This gives $qd_{\mathrm{F}} \approx \pi - \arctan(p/q)$ and the first 0-π transition occurs at $\pi/2 < qd_{\mathrm{F}} < \pi$. For a large exchange energy $H \gg T_{\mathrm{c}}$, we obtain $p \approx (1 + \omega/2\,H)/\xi_{\mathrm{H}}$ and $q \approx (1 - \omega/2\,H)/\xi_{\mathrm{H}}$. When we assume $p \approx q$, the first 0-π transition occurs at $d_{\mathrm{F}}/\xi_{\mathrm{H}} \approx 3\pi/4$, that is $d_{\mathrm{F}}/\xi_{\mathrm{F}} \approx 3\pi/\sqrt{8\,h} \approx 0.6$, which is in good agreement with figures 2(a) and (e).

By adding normal layers in the case of γ_{SN}, $\gamma_{\mathrm{NF}} \ll 1$, we see that even for two extra layers in the SNFNS configuration, the critical current density

$$J_{\mathrm{c}} \sim \sum_{\omega}\left[\frac{\Delta^2}{\omega^2}\frac{1}{\cosh^2\left(k_{\mathrm{N}}d_{\mathrm{N}}\right)}\,\mathrm{Re}\,\frac{k_{\mathrm{F}}}{\sinh\left(k_{\mathrm{F}}d_{\mathrm{F}}\right)}\right] \tag{27}$$

does not differ much from (25). We only obtain an additional real factor $\cosh^{-2}(k_{\mathrm{N}}d_{\mathrm{N}})$, but the position of the 0-π transitions is still defined by the term marked as the real part. Therefore, the positions of the 0-π transitions will be the same as in the SFS case (see figure 2(a)) for one extra N layer. The small boundary parameter γ_{SN} is needed in order to neglect the proximity effect in the S electrodes.

However, if $\gamma_{\mathrm{NF}} = 1$ in the SNFS junction (dashed-dotted line in figure 2(e)), the electrons may easily change between the N and F layers, since $\gamma_{\mathrm{NF}} \sim \sqrt{D_{\mathrm{F}}/D_{\mathrm{N}}}$. Therefore, the Josephson phase drops partially along the N layer and the first 0-π transition shifts towards smaller values of d_{F}.

3.2. Double-barrier structures SIFIS versus SINFNIS

In order to discuss the interplay of the N and I layers we jump to the description of the configurations shown by figure 2(d) and (h). Here the resistance of the insulating barriers is large γ_{BSF}, $\gamma_{\mathrm{BSN}} \gg 1$, but the NF boundaries are still transparent $\gamma_{\mathrm{BNF}} \ll 1$, and we do not need any assumption about the temperature to use the linear approximation.

The critical current density of the SIFIS junction (cf solid black lines) at $\gamma_{\mathrm{BSF}} \gg 1$ is

$$J_{\mathrm{c}} \sim \sum_{\omega}\left[\frac{\Delta^2}{\gamma_{\mathrm{BSF}}^2\xi_{\mathrm{F}}^2\sqrt{\omega^2+\Delta^2}}\,\mathrm{Re}\,\frac{1}{k_{\mathrm{F}}\sinh\left(k_{\mathrm{F}}d_{\mathrm{F}}\right)}\right]. \tag{28}$$

The points of the 0-π transitions are now defined by the solutions of the equation

$$\tan\left(qd_{\mathrm{F}}\right) = \frac{p}{q}\tanh\left(pd_{\mathrm{F}}\right). \tag{29}$$

Here the assumption $p \approx q$ yields only $d_{\mathrm{F}} = 0$. At a large exchange energy $H \gg T_{\mathrm{c}}$, the first 0-π transition occurs at $d_{\mathrm{F}}/\xi_{\mathrm{H}} < \pi/2$, that is, $d_{\mathrm{F}}/\xi_{\mathrm{F}} < \pi/\sqrt{8\,h} \approx 0.2$, which is in agreement with figures 2(d) and (h). Its exact position is defined by the factor T/H as well as γ_{BSF} [53].

In the case of intermediate resistances $\gamma_{\mathrm{BSF}} \sim 1$ of the SF interfaces of an SFS JJ [3], the critical current density reads

$$J_{\mathrm{c}} \sim \sum_{\omega}\left[\frac{\Delta^2}{\omega^2} \times \mathrm{Re}\,\frac{k_{\mathrm{F}}}{\sinh\left(k_{\mathrm{F}}d_{\mathrm{F}}\right)\left(1 + k_{\mathrm{F}}^2\xi_{\mathrm{F}}^2\Gamma^2\right) + 2k_{\mathrm{F}}\xi_{\mathrm{F}}\Gamma\cosh\left(k_{\mathrm{F}}d_{\mathrm{F}}\right)}\right], \tag{30}$$

which transforms into the two previous cases (25) and (28) for $\Gamma \equiv \gamma_{\mathrm{SF}}\sqrt{\omega^2+\Delta^2}/|\omega| \ll$ and $\gg 1$, respectively. The points of the 0-π transitions are defined by

$$\tan\left(qd_{\mathrm{F}}\right) = \frac{p\left(1 + 2\Gamma^2\right)\tanh\left(pd_{\mathrm{F}}\right) + 4p\Gamma}{q\left(1 - 2\Gamma^2\right)}. \tag{31}$$

If $2\Gamma > 1$, that is, $\gamma_{\mathrm{BSF}} > |\pi T|/\sqrt{2(\pi^2T^2+\Delta^2)}$, the first 0-$\pi$ transition is located in the range $\pi/2 < d_{\mathrm{F}}/\xi_{\mathrm{H}} < 3\pi/4$. If $\gamma_{\mathrm{BSF}} < |\pi T|/\sqrt{2(\pi^2T^2+\Delta^2)}$, it occurs at $0 < d_{\mathrm{F}}/\xi_{\mathrm{H}} < \pi/2$.

In contrast, the critical current density of the SINFNIS junction at $\gamma_{\mathrm{BSN}} \gg 1$, at transparent NF interfaces $\gamma_{\mathrm{BNF}} \ll 1$ and $\gamma_{\mathrm{NF}} \ll 1$, has the form

$$J_{\mathrm{c}} \sim \sum_{\omega}\left[\frac{\Delta^2}{\sqrt{\omega^2+\Delta^2}}\frac{1}{\gamma_{\mathrm{BNF}}^2\xi_{\mathrm{N}}^2k_{\mathrm{N}}^2\sinh^2\left(k_{\mathrm{N}}d_{\mathrm{N}}\right)} \times \mathrm{Re}\,\frac{k_{\mathrm{F}}}{\sinh\left(k_{\mathrm{F}}d_{\mathrm{F}}\right)}\right]. \tag{32}$$

The 0-π transitions are defined by the zeros of the real part, which has the same form as in the case of SFS JJs with transparent interfaces (25). That is, the N layers have mitigated the effect of the I layers, which can be seen by comparing figures 2(d) with (a).

3.3. SIFIS versus SINFIS structures

The effect of a single N layer on a double-barrier SIFIS junction, shown in figure 2(c) and (g), is discussed in the following. The critical current density of the SINFIS junction with the same boundary parameters as in the section before is given by

$$J_c \sim \sum_{\omega} \left[\frac{\Delta^2}{\sqrt{\omega^2+\Delta^2}} \frac{1}{\gamma_{BNF}^2 \xi_N k_N \sinh\left(k_N d_N\right)} \times \mathrm{Re}\, \frac{k_F}{\cosh\left(k_F d_F\right)} \right]. \tag{33}$$

In this case, the 0-π transitions are defined by the zeros of the function $\cos(qd_F)$ and located at the positions where $d_F/\xi_H = \pi/2 + \pi m$, $m = 0, 1, 2 \ldots$; that is, they are also shifted towards larger d_F in comparison with the ones of the SIFIS junction; see figures 2(c) and (g).

In our previous article [42] we obtained in fact the same expressions (28) and (33). There we assumed that the interface transparencies of both S electrodes are small, one of them due to the presence of an insulating barrier. In this way we analysed SI_1FI_2S and SI_1NFI_2S structures with rather different transparencies of the I_1 and I_2 barriers. We found in the linear approximation that the critical current density for an SI_1NFI_2S FJJ is the same as the one for an SI_1FNI_2S structure.

3.4. SIFS versus SINFS structures

If the structure contains only one insulating barrier, as in figure 2(b) and (f), we may use the tunnel Hamiltonian method, which, for the critical current density, yields the expression

$$J_c \sim \sum_{\omega} \frac{\Delta^2}{\sqrt{\omega^2+\Delta^2}} \mathrm{Re} \sin\theta_{N,S}. \tag{34}$$

To use the linear approximation we shall assume that T is close to T_c, and in order to neglect the proximity effect in the right S electrode we use the rigid boundary conditions γ_{BSF}, $\gamma_{SF} \ll 1$. We also assume the N layer to be thin, $d_N \ll \xi_N$. Then we obtain

$$\theta_{N,S} = \frac{1 + \gamma_{NF} \frac{\xi_F k_F}{\sinh k_F d_F} \left(\frac{d_N}{\xi_N} \cosh k_F d_F + \gamma_{BSN} \right)}{1 + \gamma_{NF} \frac{\xi_F k_F \cosh k_F d_F}{\sinh k_F d_F} \left(\frac{d_N}{\xi_N} + \gamma_{BSN} \right)}. \tag{35}$$

To find the position of the first 0-π transition we assume $d_F \sim \xi_H$ and neglect $d_N/\xi_N \ll \gamma_{BSN}$, because the last value is determined by the large resistance of the I barrier. The solution weakly depends on d_N because the suppression of the superconducting correlation along the thin N layer is negligible in comparison with that of the I barrier. However, the ratio of the N and F resistance, which defines via γ_{NF} (the derivative jump (10) at the NF interface), still plays a role. Then the 0-π transition takes place at d_F, for which the equation

$$1 + \gamma + 2\gamma^2 \cos\frac{d_F}{\xi_H} + \gamma\left(\cos\frac{d_F}{\xi_H} + \sin\frac{d_F}{\xi_H} \right) = 0 \tag{36}$$

is satisfied.

If $\gamma \equiv \gamma_{BSN}\gamma_{NF}\xi_F/\xi_H \gg 1$, the main term gives $\cos(d_F/\xi_H) = 0$ and $d_F/\xi_H = \pi/2$, which corresponds to the solution for the SIFS FJJ [28]. If $\gamma \gtrsim 1$, the position of the 0-π transition shifts towards larger d_F depending on $\gamma \sim \gamma_{NF}$; see figure 2(f). If $\gamma \ll 1$ we cannot use this approach, assuming large γ_{BSN}.

4. Comparison with experiment

To check our theory, we use data from SINFS JJs [26], based on $Nb|Al_2O_3|Cu|Ni_{0.6}Cu_{0.4}|Nb$ heterostructures. These samples include a 2 nm Cu interlayer between the I and F layers. Using the same technology, new series of samples were produced, but the process was changed in order to delete the Cu layer. That is, we can compare SIFS and SINFS FJJs with the same layer properties, including the concentration of the NiCu alloy. In figure 4 we show a fit of experimental data of critical current densities for different F layer thicknesses d_F of both types of junctions. Dots correspond to SIFS junctions and triangles correspond to SINFS junctions.

We calculated the critical current densities with the help of (18). In the case of the SIFS configuration we made use of (20) to calculate the parameter χ^- and in the case of the SINFS configuration we used (22). For our

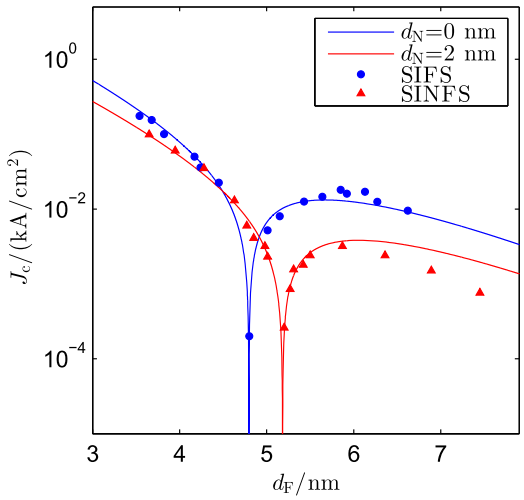

Figure 4. The critical current density (18) fitted to the experimental data of SIFS junctions and SINFS junctions. For the calculation of χ^- in the SIFS case we used (20), and in the SINFS case we used (22). Fitting parameters are $\gamma_{BSN} = 90000$, $\gamma_{BNF} = 0.01$, $\gamma_{BSF} = 0.1$ and $\gamma_{NF} = 0.016$.

fit we used the coherence lengths $\xi_N = 10$ nm, $\xi_F = 7.60$ nm and $\xi_H = 1.72$ nm. Our exchange energy $H/k_B = 880$ K is situated between the value 850 K corresponding to the alloy $Ni_{0.53}Cu_{0.47}$ [27] and the value 930 K of clean Ni [36]. The product $\tau_m H = 1/1.7$ is similar to the one used by Weides *et al* [26]. Further values taken from this publication are the temperature T = 4.2 K, junction area $A = (100\,\mu\,\mathrm{m})^2$ and resistivity $\rho_F = 54\,\mu\Omega$cm. Additionally, we used the damped critical temperature $T_c = 7.2$ K of Nb and the resistivity $\rho_N = 0.66\,\mu\Omega$cm. Together with the fit parameters $\gamma_{BSF} = 0.1$, $\gamma_{BSN} = 90000$, $\gamma_{BNF} = 0.01$ and $\gamma_{NF} = 0.016$ of figure 4 we obtain the boundary resistances $R_{BSF} = 4.10$ nΩ, $R_{BSN} = 584\,\mu\Omega$ and $R_{BNF} = 0.41$ nΩ, which are realistic values.

As we have shown in figure 2(f), a small suppression parameter $\gamma_{NF} < 1$ results in a shift of the 0-π transition to larger d_F for the sample with N layer. This effect explains the shift of the 0-π transition observed in the experiments on SIFS and SINFS FJJs. The difference in the amplitude of the curves is attributed to the different thicknesses of the I barrier in these two sample series.

This conclusion is also supported by experimental observations on SIsFS junctions [54–56]. These observations indicate that the introduction of a thin s interlayer, which should make a transition to the normal state if its thickness is of the order of the coherence length, shifts the 0-π transitions towards larger d_F.

5. Conclusion

Using the Usadel equations, we have calculated the critical current densities of ferromagnetic Josephson junctions (FJJs) of different types, containing I and N layers at the SF interfaces, and compared them to critical current densities of structures without N layers. Such layers were technologically required in many FJJ experiments, but were not taken into account in previous models.

It was shown earlier [28, 52, 53] that insulating barriers decrease the critical current density and shift the 0-π transitions to smaller values of the ferromagnet thickness d_F. A thin N layer inserted between S and I layers does not significantly influence the Josephson effect. However, if the N layer is inserted between I and F layers, it can have a large effect on the $J_c(d_F)$ curve. Additionally, if the transport properties of the F and N layers differ significantly ($\gamma_{NF} \ll 1$), the presence of the N layer shifts the first 0-π transition to larger d_F; see figures 2(b)–(d). At certain values of d_F, the 0-π transition can even be achieved by changing only d_N; see figure 3. Finally, our theory allows the explanation of experimental data for SINFS and SIFS junctions, shown in figure 4.

In comparison with simple SFS JJs, the oscillation period of $J_c(d_F)$ in the dirty limit is still determined by the magnetic exchange energy H and the diffusion coefficient D_F. However, the positions of $J_c(d_F)$ minima are shifted because of different boundary conditions. When the dirty limit does not apply, the oscillation period of $J_c(d_F)$ may depend on many other parameters and does not have to be constant, but can change with the F layer thickness [57]. A multi-domain structured ferromagnet may also change $J_c(d_F)$; for instance, the oscillation period decreases when the domain width increases [58].

If the transport properties of the N layer between the I and F layer are the same as those of the ferromagnet, not only the period of the $J_c(d_F)$ dependence stays the same as in SFS, but also its position (d_F of the 1st minimum). Thus, the dead layer [24, 26, 30–34] changes the position of $J_c(d_F)$ minima only if its transport

properties differ from those of the F layer. The smaller the value of γ_{NF}, the larger is the change of the J_c amplitude and the shift of the 0-π transitions; see figures 2(f)–(h).

The situation is completely different in the case of transparent SF interfaces, that is, without an I layer in between. In this case, the additional thin normal layer with conductivity much larger than that of the ferromagnet ($\gamma_{NF} \ll 1$) does not play any role. In the same setup, an N layer with transport properties similar to those of the ferromagnet ($\gamma_{NF} \approx 1$) provides a shift of the 0-π transitions to smaller d_F; see figure 2(e). This process is explained in more detail after (24).

In summary, even a thin additional N layer may change the boundary conditions at the IF boundary depending on the value of γ_{NF}. We conclude that it can effectively mitigate the effect of the insulating barrier on the decaying oscillations of the critical current density $J_c(d_F)$. Even technological thin N layers, which do not quite suppress the superconducting correlations, have to be considered carefully when including them into novel superconducting–magnetic hybrid devices.

Acknowledgments

We thank Professor V V Ryazanov for fruitful and stimulating discussions. NGP thanks the CMPC RHUL for giving new ideas in stimulating discussions, and DMH thanks Professor W P Schleich and K Vogel for giving him the opportunity to work at the Lomonosov Moscow State University. Financial support by the DFG (Projects SFB/TRR-21 and KO 1953/11-1) and Open Access Publishing Fund of the University of Tübingen, the EPSRC (grant No. EP/J010618/1), the Russian Foundation for Basic Researches (RFBR grants Nos 13-02-01452-a, 14-02-90018-Bel-a) and the Ministry of Education and Science of Russian Federation (grant No. 14Y26.31.0007) is gratefully acknowledged.

Appendix. N layer Green's function

In this appendix we first show how to find the dependence of $\theta_{N,F}$ on $\chi_N \equiv \sin(\theta_{F,N}/2)$ in order be able to solve (22) numerically for χ_N. Thereafter, we reduce (22) in the limiting case η, $\gamma_{NF} \to 0$ to an equation of fourth order in χ_N.

We start by solving the Usadel equation (4) in the case $j = N$, that is

$$\xi_N^2 \frac{\partial^2}{\partial x^2}\theta_N(x) = \Omega \sin\theta_N(x), \tag{A.1}$$

where $\Omega \equiv \omega/(\pi T_c)$ because the exchange energy h is zero in the N layer.

When we assume $\xi_N \gg d_N$, the function $\theta_N(x)$ changes only slowly. Therefore, in the right-hand side of (A.1) we make the approximation

$$\sin\theta_N(x) \approx \sin\theta_{N,S} \equiv \text{const}, \tag{A.2}$$

where $\theta_{N,S} \equiv \theta_N(x_{SN})$. Note that we cannot neglect this term because $\theta_N(x)$ may be of the order of θ_S, depending on the boundary parameters. The solution of (A.1) using the approximation (A.2) reads

$$\theta_N(x) = \frac{\Omega}{2\xi_N^2}\sin\theta_{N,S}\left(x - x_{SN}\right)^2 + a\left(x - x_{SN}\right) + \theta_{N,S}. \tag{A.3}$$

Inserting the constant

$$a = \frac{1}{\gamma_{BSN}\xi_N}\sin\left(\theta_{N,S} - \theta_S\right), \tag{A.4}$$

determined from the the boundary condition (8) at the SN interface, into the Green's function (A.3) at the position x_{NF} connects the NF boundary value

$$\theta_{N,F} = \frac{\Omega d_N^2}{2\xi_N^2}\sin\theta_{N,S} + \frac{d_N}{\gamma_{BSN}\xi_N}\sin\left(\theta_{N,S} - \theta_S\right) + \theta_{N,S} \tag{A.5}$$

to the SN boundary value $\theta_{N,S}$, which we determine in the next step.

For this purpose we use the integrated sine-Gordon equation (14) at the position x_{NF} and insert it into the differentiability condition (10) to obtain

$$-2\gamma_{NF}\sqrt{\widetilde{\Omega} + \eta\cos^2\frac{\theta_{F,N}}{2}}\sin\frac{\theta_{F,N}}{2} = \xi_N\left[\frac{\partial}{\partial x}\theta_N\right]_{x_{NF}}. \tag{A.6}$$

Here we replace the right-hand side with the derivative

$$\left[\frac{\partial\theta_{\mathrm{N}}}{\partial x}\right]_{x_{\mathrm{NF}}} = \frac{\Omega d_{\mathrm{N}}}{\xi_{\mathrm{N}}^2}\sin\theta_{\mathrm{N,S}} + \frac{\sin\left(\theta_{\mathrm{N,S}} - \theta_{\mathrm{S}}\right)}{\gamma_{\mathrm{BSN}}\xi_{\mathrm{N}}} \tag{A.7}$$

of the function $\theta_{\mathrm{N}}(x)$ from (A.3).

These steps lead us with the definition $\chi_{\mathrm{N}} \equiv \sin(\theta_{\mathrm{F,N}}/2)$ to

$$-2\gamma_{\mathrm{NF}}\gamma_{\mathrm{BSN}}\sqrt{\widetilde{\Omega} + \eta\left(1 - \chi_{\mathrm{N}}^2\right)}\,\chi_{\mathrm{N}} = \Omega\frac{d_{\mathrm{N}}}{\xi_{\mathrm{N}}}\gamma_{\mathrm{BSN}}\sin\theta_{\mathrm{N,S}} + \sin\left(\theta_{\mathrm{N,S}} - \theta_{\mathrm{S}}\right). \tag{A.8}$$

This equation can be written as an equation of second order in $\mu \equiv \sin\theta_{\mathrm{N,S}}$ and can therefore be solved exactly for $\theta_{\mathrm{N,S}}$. Inserting the result into (A.5) gives us $\theta_{\mathrm{N,F}}$ as a function of χ_{N}, which itself, when inserted into (22), allows us to finally determine χ_{N} by solving the transcendental equation (22) numerically.

In the following we consider the limit $\eta,\ \gamma_{\mathrm{NF}} \to 0$ to reduce (22) to an equation of fourth order in χ_{N}. This limit allows us to neglect the term containing χ_{N} in (A.8). Together with the definition (A.4), we obtain the equation

$$\sin\theta_{\mathrm{N,S}} = -\frac{\xi_{\mathrm{N}}^2}{\Omega d_{\mathrm{N}}}a, \tag{A.9}$$

which we use to replace $\theta_{\mathrm{N,S}}$ in (A.4).

Solving the resulting equation for a and re-inserting it into (A.9) leads us to the expression

$$\sin\theta_{\mathrm{N,S}} = \lambda\sin\theta_{\mathrm{S}}, \tag{A.10}$$

where we used the definition

$$\lambda \equiv \left(1 + 2\cos\theta_{\mathrm{S}}\gamma_{\mathrm{BSN}}\frac{\Omega d_{\mathrm{N}}}{\xi_{\mathrm{N}}} + \gamma_{\mathrm{BSN}}^2\frac{\Omega^2 d_{\mathrm{N}}^2}{\xi_{\mathrm{N}}^2}\right)^{-1/2}. \tag{A.11}$$

With the help of (A.10) we replace $\theta_{\mathrm{N,S}}$ in (A.5), which in turn is used in (22) to reduce it finally together with $\eta \to 0$ to an equation of fourth order in χ_{N}.

References

[1] Linder J and Robinson J W A 2015 *Nat. Phys.* **11** 307–15
[2] Golubov A A, Kupriyanov M Yu and Il'ichev E 2004 *Rev. Mod. Phys.* **76** 411–69
[3] Buzdin A I 2005 *Rev. Mod. Phys.* **77** 935–76
[4] Bergeret F S, Volkov A F and Efetov K B 2005 *Rev. Mod. Phys.* **77** 1321–73
[5] Holmes D S, Ripple A L and Manheimer M A 2013 *IEEE Trans. Appl. Supercond.* **23** 1701610
[6] Manheimer M A 2015 *IEEE Trans. Appl. Supercond.* **25** 1–4
[7] Ioffe L B, Geshkenbein V B, Feigel'man M V, Fauchère A L and Blatter G 1999 *Nature* **398** 679–81
[8] Ustinov A V and Kaplunenko V K 2003 *J. Appl. Phys.* **94** 5405–7
[9] Yamashita T, Takahashi S and Maekawa S 2006 *Appl. Phys. Lett.* **88** 132501
[10] Ortlepp T, Ariando, Mielke O, Verwijs C J M, Foo K F K, Rogalla H, Uhlmann F H and Hilgenkamp H 2006 *Science* **312** 1495–7
[11] Klenov N, Kornev V, Vedyayev A, Ryzhanova N, Pugach N and Rumyantseva T 2008 *J. Phys. Conf. Ser.* **97** 012037
[12] Feofanov A K *et al* 2010 *Nat. Phys.* **6** 593–7
[13] Vernik I V, Bol'ginov V V, Bakurskiy S V, Golubov A A, Kupriyanov M Yu, Ryazanov V V and Mukhanov O A 2013 *IEEE Trans. Appl. Supercond.* **23** 1701208
[14] Goldobin E, Sickinger H, Weides M, Ruppelt N, Kohlstedt H, Kleiner R and Koelle D 2013 *Appl. Phys. Lett.* **102** 242602
[15] Zdravkov V I, Lenk D, Morari R, Ullrich A, Obermeier G, Müller C, Krug von Nidda H A, Sidorenko A S, Horn S, Tidecks R and Tagirov L R 2013 *Appl. Phys. Lett.* **103** 062604
[16] Bakurskiy S V, Klenov N V, Soloviev I I, Kupriyanov M Yu and Golubov A A 2013 *Phys. Rev.* B **88** 144519
[17] Abd el Qader M, Singh R K, Galvin S N, Yu L, Rowell J M and Newman N 2014 *Appl. Phys. Lett.* **104** 022602
[18] Niedzielski B M, Diesch S G, Gingrich E C, Wang Yixing, Loloee R, Pratt W P and Birge N O 2014 *IEEE Trans. Appl. Supercond.* **24** 1–7
[19] Alidoust M and Halterman K 2014 *Phys. Rev.* B **89** 195111
[20] Baek B, Rippard W H, Benz S P, Russek S E and Dresselhaus P D 2014 *Nat. Commun.* **5** 3888
[21] Bakurskiy S V, Gudkov A L, Klenov N V, Kuznetsov A V, Kupriyanov M Yu and Soloviev I I 2014 *Moscow Univ. Phys. Bull.* **69** 275–86
[22] Soloviev I I, Klenov N V, Bakurskiy S V, Bol'ginov V V, Ryazanov V V, Kupriyanov M Yu and Golubov A A 2014 *Appl. Phys. Lett.* **105** 242601
[23] Baek B, Rippard W H, Pufall M R, Benz S P, Russek S E, Rogalla H and Dresselhaus P D 2015 *Phys. Rev. Appl.* **3** 011001
[24] Oboznov V A, Bol'ginov V V, Feofanov A K, Ryazanov V V and Buzdin A I 2006 *Phys. Rev. Lett.* **96** 197003
[25] Kontos T, Aprili M, Lesueur J, Genêt F, Stephanidis B and Boursier R 2002 *Phys. Rev. Lett.* **89** 137007
[26] Weides M, Kemmler M, Goldobin E, Koelle D, Kleiner R, Kohlstedt H and Buzdin A 2006 *Appl. Phys. Lett.* **89** 122511
[27] Ryazanov V V, Oboznov V A, Rusanov A Yu, Veretennikov A V, Golubov A A and Aarts J 2001 *Phys. Rev. Lett.* **86** 2427
[28] Vasenko A S, Golubov A A, Kupriyanov M Yu and Weides M 2008 *Phys. Rev.* B **77** 134507
[29] Buzdin A 2003 *Pis'ma Zh. Eksp. Teor. Fiz.* **78** 1073–76
Buzdin A 2003 *JETP Lett.* **78** 583–86 (Engl. transl.)
[30] Blum Y, Tsukernik A, Karpovski M and Palevski A 2002 *Phys. Rev. Lett.* **89** 187004

[31] Sellier H, Baraduc C, Lefloch F and Calemczuk R 2003 *Phys. Rev.* B **68** 054531
[32] Weides M, Kemmler M, Kohlstedt H, Waser R, Koelle D, Kleiner R and Goldobin E 2006 *Phys. Rev. Lett.* **97** 247001
[33] Pfeiffer J, Kemmler M, Koelle D, Kleiner R, Goldobin E, Weides M, Feofanov A K, Lisenfeld J and Ustinov A V 2008 *Phys. Rev.* B **77** 214506
[34] Bannykh A A, Pfeiffer J, Stolyarov V S, Batov I E, Ryazanov V V and Weides M 2009 *Phys. Rev.* B **79** 054501
[35] Born F, Siegel M, Hollmann E K, Braak H, Golubov A A, Gusakova D Yu and Kupriyanov M Yu 2006 *Phys. Rev.* B **74** 140501
[36] Robinson J W A, Piano S, Burnell G, Bell C and Blamire M G 2006 *Phys. Rev. Lett.* **97** 177003
[37] Robinson J W A, Piano S, Burnell G, Bell C and Blamire M G 2007 *Phys. Rev.* B **76** 094522
[38] Wild G, Probst C, Marx A and Gross R 2010 *Eur. Phys. J.* B **78** 509–23
[39] Fominov Ya V, Schumann J, Hess C, Kataev V, Büchner B and Garifullin I A 2015 *Phys. Rev.* B **91** 214508
[40] Golubov A A, Kupriyanov M Yu and Fominov Ya V 2002 *Pis'ma Zh. Eksp. Teor. Fiz.* **75** 223–7
Golubov A A, Kupriyanov M Yu and Fominov Ya V 2002 *JETP Lett.* **75** 190–4 (Engl. transl.)
[41] Golubov A A and Kupriyanov M Yu 2005 *Pis'ma Zh. Eksp. Teor. Fiz.* **81** 419–25
Golubov A A and Kupriyanov M Yu 2005 *JETP Lett.* **81** 335–41 (Engl. transl.)
[42] Pugach N G, Kupriyanov M Yu, Vedyayev A V, Lacroix C, Goldobin E, Koelle D, Kleiner R and Sidorenko A S 2009 *Phys. Rev.* B **80** 134516
[43] Liu J-F and Chan K S 2010 *Phys. Rev.* B **82** 184533
[44] Vasenko A S, Kawabata S, Golubov A A, Kupriyanov M Yu and Hekking F W J 2010 *Physica* C **470** 863–66
[45] Vasenko A S, Kawabata S, Golubov A A, Kupriyanov M Yu, Lacroix C, Bergeret F S and Hekking F W J 2011 *Phys. Rev.* B **84** 024524
[46] Ryazanov V V, Oboznov V A, Bol'ginov V V and Rossolenko A N 2008 *Proc. of XII Int. Symp. Nanophysics and Nanoelectronics* vol 1 (Nizhniy Novgorod: IFM RAS) p 42 (in Russian)
[47] Usadel K D 1970 *Phys. Rev. Lett.* **25** 507–9
[48] Zaikin A D and Zharkov G F 1981 *Fiz. Nizk. Temp.* **7** 375–9
Zaikin A D and Zharkov G F 1981 *Sov. J. Low Temp. Phys.* **7** 184–8 (Engl. transl.)
[49] Kuprianov M Yu and Lukichev V F 1988 *Zh. Eksp. Teor. Fiz.* **94** 139–49
Kuprianov M Yu and Lukichev V F 1988 *Sov. Phys. JETP* **67** 1163–8 (Engl. transl.)
[50] Koshina E A and Krivoruchko V N 2000 *Low Temp. Phys.* **26** 115–20
[51] Buzdin A I and Kupriyanov M Yu 1991 *Pis'ma Zh. Eksp. Teor. Fiz.* **53** 308–12
Buzdin A I and Kupriyanov M Yu 1991 *JETP Lett.* **53** 321–6 (Engl. transl.)
[52] Fauré M, Buzdin A I, Golubov A A and Kupriyanov M Yu 2006 *Phys. Rev.* B **73** 064505
[53] Buzdin A and Baladié I 2003 *Phys. Rev.* B **67** 184519
[54] Bakurskiy S V, Klenov N V, Soloviev I I, Bol'ginov V V, Ryazanov V V, Vernik I V, Mukhanov O A, Kupriyanov M Yu and Golubov A A 2013 *Appl. Phys. Lett.* **102** 192603
[55] Larkin T I, Bol'ginov V V, Stolyarov V S, Ryazanov V V, Vernik I V, Tolpygo S K and Mukhanov O A 2012 *Appl. Phys. Lett.* **100** 222601
[56] Ruppelt N, Sickinger H, Menditto R, Goldobin E, Koelle D, Kleiner R, Vavra O and Kohlstedt H 2015 *Appl. Phys. Lett.* **106** 022602
[57] Pugach N G, Kupriyanov M Yu, Goldobin E, Kleiner R and Koelle D 2011 *Phys. Rev.* B **84** 144513
[58] Bakurskiy S V, Golubov A A, Klenov N V, Kupriyanov M Yu and Soloviev I I 2015 *JETP Lett.* **101** 765–71